

## Research Article

# Analysis of Thermal Stability in a Convecting and Radiating Two-Step Reactive Slab

O. D. Makinde and M. S. Tshehla

*Faculty of Military Science, Stellenbosch University, Private Bag X2, Saldanha 7395, South Africa*

Correspondence should be addressed to O. D. Makinde; makinded@gmail.com

Received 27 February 2013; Revised 20 July 2013; Accepted 26 September 2013

Academic Editor: Akhilendra Singh

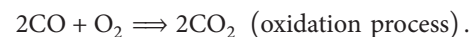
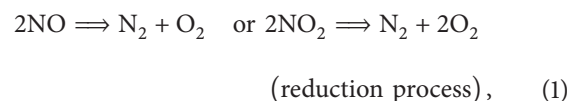
Copyright © 2013 O. D. Makinde and M. S. Tshehla. This is an open access article distributed under the Creative Commons Attribution License, which permits unrestricted use, distribution, and reproduction in any medium, provided the original work is properly cited.

This paper investigates the combined effects of convective and radiative heat loss on thermal stability of a rectangular slab of combustible materials with internal heat generation due to a two-step exothermic chemical reaction, taking the diffusion of the reactant into account and assuming a variable (temperature dependent) preexponential factor. The nonlinear differential equation governing the transient reaction-diffusion problem is obtained and tackled numerically using a semidiscretization finite difference technique. A special type of Hermite-Padé approximants coupled with perturbation technique are employed to analyze the effects of various embedded thermophysical parameters on the steady state problem. Important properties of the temperature field including thermal stability conditions are presented graphically and discussed quantitatively.

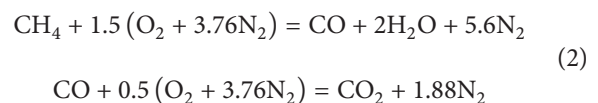
## 1. Introduction

Analysis of thermal stability in a reactive slab of combustible materials due to exothermic chemical reaction plays a significant role in improving the design and operation of many industrial and engineering devices and find applications in power production, jet and rocket propulsion, fire prevention and safety, pollution control, material processing industries, and so on [1]. For instance, solid propellants used in rocket vehicles are capable of experiencing exothermic reactions without the addition of any other reactants. The theory of thermal stability of reactive materials has long been a fundamental topic in the field of combustion [2]. It is directly related to the determination of critical regimes separating the regions of explosive and nonexplosive ways of chemical reactions (Frank Kamenetskii [3]). The chemical reaction may be modelled by considering either a single step or multistep reaction kinetics. For instance, catalytic converter used in an automobile's exhaust system provides a platform for a two-step exothermic chemical reaction where unburned hydrocarbons completely combust. This helps to reduce the emissions of toxic car pollutant such as carbon monoxide (CO) into the environment. The main

chemical reaction schemes in an autocatalytic converter are [4, 5]



Similarly, the combustion taking place within  $k$ -fluid is treated as a two-step irreversible chemical reaction of methane oxidation as follows [6]:



The vast majority of studies on thermal stability of chemically reactive materials have been concerned with homogeneous boundary conditions ranging from the infinite Biot number case [7, 8] (Frank-Kamenetskii conditions) to a range of Biot numbers [9, 10] (Semenov conditions). Previous

investigations have included a variety of geometries and have been directed towards obtaining critical conditions for thermal ignition to occur, in the form of a critical value for the Frank-Kamenetskii parameter [11]. Mathematical models of the problem relating to exothermic reaction in a reactive slab may be extremely stiff owing to the temperature dependence of the chemical reactions. Moreover, the differential equation for the temperature distribution in a convective-radiative reactive slab with temperature dependent preexponential factor is highly nonlinear and does not admit an exact analytical solution. Consequently, the equation has been solved either numerically or using a variety of approximate semianalytical methods. The preceding literature clearly shows that the work on reacting slab has been confined to convective surface heat loss. No attempt has been made to study the combined effects of convective and radiative heat losses at the slab surface despite its relevance in various technological applications such as aerothermodynamic heating of spaceships and satellites, nuclear reactor thermohydraulics, and glass manufacturing. Thermal radiation is characteristic of any material system at temperatures above the absolute zero and becomes an important form of heat transfer in devices that operate at high temperatures. Radiation is the dominant form of heat transfer in applications such as furnaces, boilers, and other combustion systems.

The present investigation aims to extend the recent work of Makinde [12] to include combined effects of convective and radiative heat losses on slab of combustible materials with internal heat generation due to a two-step exothermic reaction. Although, combustion process consists of series of chemical reactions, the choice of two-step reaction process in this study will enhance better understanding on thermal effects of chemical kinetic involving oxidation and reduction of exothermic reactions [6] in particular as well as multistep combustion process in general. Both the transient and the steady state problems are tackled numerically using semidiscretization finite difference method [13] and a special type of Hermite-Padé approximants coupled with perturbation technique [8, 9, 14]. The critical regime separating the regions of explosive and nonexplosive ways of a two-step exothermic chemical reactions is determined. It is hoped that the results obtained will not only provide useful information for applications but also serve as a complement to the previous studies.

## 2. Mathematical Model

The dynamical thermal behaviour of a rectangular slab of combustible materials with internal heat generation due to a two-step exothermic chemical reaction, taking into account the diffusion of the reactant and the temperature dependent variable preexponential factor, is considered. It is assumed that the slab surface is subjected to both convective and radiative heat losses to the environment. The geometry of the problem is depicted in Figure 1. It is assumed that the slab surface is subjected to both convective and radiative heat losses to the environment.

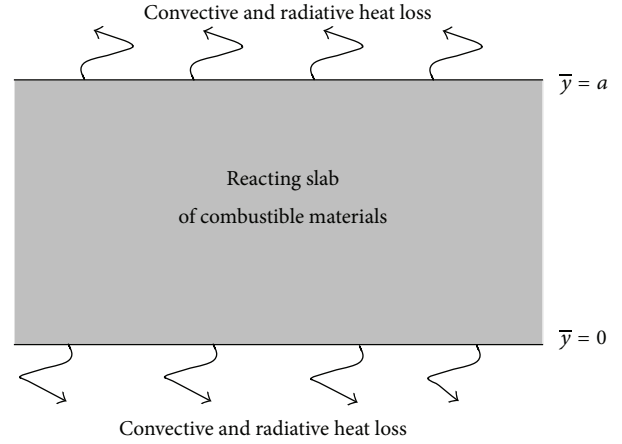


FIGURE 1: Sketch of the physical model.

The one-dimensional heat balance equation in the original variables together with the initial and boundary conditions can be written as [1, 8–12]

$$\begin{aligned} \rho c_p \frac{\partial T}{\partial \bar{t}} &= k \frac{\partial^2 T}{\partial \bar{y}^2} + Q_1 C_1 A_1 \left( \frac{KT}{vg} \right)^m e^{-(E_1/RT)} \\ &+ Q_2 C_2 A_2 \left( \frac{KT}{vg} \right)^m e^{-(E_2/RT)} - \varepsilon \sigma [T - T_\infty^4], \\ T(\bar{y}, 0) &= T_0, \\ k \frac{\partial T}{\partial \bar{y}}(0, \bar{t}) &= h_1 [T(0, \bar{t}) - T_\infty], \\ k \frac{\partial T}{\partial \bar{y}}(a, \bar{t}) &= -h_2 [T(a, \bar{t}) - T_\infty] \quad \text{for } \bar{t} > 0, \end{aligned} \quad (3)$$

where  $T$  is the absolute temperature,  $T_0$  is the initial temperature,  $T_\infty$  is the ambient temperature,  $\bar{t}$  is the time,  $h$  is the convective heat transfer coefficient,  $k$  is the thermal conductivity of the material,  $\varepsilon$  is the slab surface emissivity,  $\sigma$  is the Stefan-Boltzmann constant,  $Q_1$  is the first step heat of reaction,  $Q_2$  is the second step heat of reaction,  $A_1$  is the first step reaction rate constant,  $A_2$  is the second step reaction rate constant,  $E_1$  is the first step reaction activation energy,  $E_2$  is the second step reaction activation energy,  $\rho$  is the density,  $R$  is the universal gas constant,  $C_1$  is the first step reactant species initial concentration,  $C_2$  is the second step reactant species initial concentration,  $g$  is Planck's number,  $K$  is Boltzmann's constant,  $v$  is vibration frequency,  $a$  is the slab half width,  $\bar{y}$  is distance measured in the normal direction to the plane,  $c_p$  is the specific heat at constant pressure, and  $m$  is the numerical exponent such that  $m = \{-2, 0, 1/2\}$  represent numerical exponent for sensitized, Arrhenius, and bimolecular kinetics, respectively

[2, 3, 8]. The following dimensionless variables are introduced into (3)

$$\begin{aligned} \theta &= \frac{E_1(T - T_\infty)}{RT_\infty^2}, & \gamma &= \frac{RT_\infty}{E_1}, & y &= \frac{\bar{y}}{a}, \\ \beta &= \frac{Q_2 C_2 A_2}{Q_1 C_1 A_1} e^{(E_1 - E_2)/RT_\infty}, & r &= \frac{E_2}{E_1}, & \text{Bi}_1 &= \frac{ha}{k}, \\ \text{Bi}_2 &= \frac{ha}{k}, & \lambda &= \frac{E_1 a^2 Q_1 C_1 A_1}{kRT_\infty^2} \left[ \frac{KT_\infty}{\nu g} \right]^m e^{-(E_1/RT_\infty)}, \\ t &= \frac{k\bar{t}}{\rho c_p a^2}, & b &= \frac{E_1(T_0 - T_\infty)}{RT_\infty^2}, & N_r &= \frac{\varepsilon \sigma a E_1 T_\infty^3}{kR}, \end{aligned} \quad (4)$$

and we obtain the dimensionless governing equation together with initial and boundary conditions as

$$\frac{\partial \theta}{\partial t} = \frac{\partial^2 \theta}{\partial y^2} + \lambda(1 + \gamma\theta)^m \left[ e^{\theta/(1+\gamma\theta)} + \beta e^{(r\theta)/(1+\gamma\theta)} \right] \quad (5)$$

$$-N_r \left[ (\gamma\theta + 1)^4 - 1 \right], \quad \theta(y, 0) = b, \quad (6)$$

$$\frac{\partial \theta}{\partial y}(0, t) = \text{Bi}_1 \theta(0, t), \quad (7)$$

$$\frac{\partial \theta}{\partial y}(1, t) = -\text{Bi}_2 \theta(1, t) \quad \text{for } t > 0,$$

where  $\lambda$ ,  $\gamma$ ,  $\beta$ ,  $r$ ,  $b$ ,  $N_r$ ,  $\text{Bi}_1$ , and  $\text{Bi}_2$ , represent the Frank-Kamenetskii parameter, activation energy parameter, two-step exothermic reaction parameter, activation energy ratio parameter, slab of the initial temperature parameter, thermal radiation parameter, and the Biot numbers for the slab lower and upper surfaces, respectively. Initially at  $t = 0$ , the slab temperature and that of ambient are assumed to be the same; that is,  $b = 0$ . For  $t > 0$ , the exothermic reaction within the slab occurs, and the slab temperature increases above that of ambient. In the following section, (5)–(7) are solved numerically using a semidiscretization finite difference method [13].

### 3. Numerical Procedure

Here semidiscretization finite difference technique [13] is employed to tackle the model nonlinear initial boundary value problem in (5)–(7). The discretization is based on a linear cartesian mesh and uniform grid on which finite differences are taken (see Figure 2). Firstly, a partition of the spatial interval  $[0, 1]$  is introduced. We divide it into  $N$  equal parts and define grid size  $\Delta y = 1/N$  and grid points  $y_i = (i-1)\Delta y$ ,  $1 \leq i \leq N+1$ .

The first and the second spatial derivatives in (5)–(7) are approximated with second-order central differences. Let  $\theta_i(t)$

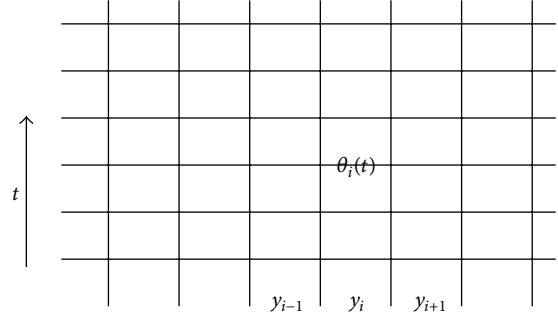


FIGURE 2: Computational domain with nodes.

be an approximation of  $\theta(y_i, t)$ ; then the semidiscrete system for the problem reads

$$\begin{aligned} \frac{d\theta_i}{dt} &= \frac{1}{(\Delta y)^2} (\theta_{i+1} - 2\theta_i + \theta_{i-1}) \\ &+ \lambda(1 + \gamma\theta_i)^m \left[ e^{\theta_i/(1+\gamma\theta_i)} + \beta e^{(r\theta_i)/(1+\gamma\theta_i)} \right] \\ &- N_r \left[ (\gamma\theta_i + 1)^4 - 1 \right], \end{aligned} \quad (8)$$

with initial conditions

$$\theta_i(0) = b, \quad 1 \leq i \leq N+1. \quad (9)$$

The equations corresponding to the first and last grid points are modified to incorporate the boundary conditions as follows:

$$\theta_{N+1} = \theta_N (1 - \Delta y \text{Bi}_2), \quad \theta_2 = \theta_1 (1 + \Delta y \text{Bi}_1). \quad (10)$$

In (8), there is only one independent variable, so they are ordinary differential equations. Since they are first order and the initial conditions for all variables are known, the problem is an initial value problem. The MATLAB program ode45 is employed to integrate sets of differential equations using a fourth-order Runge-Kutta integration scheme.

### 4. Steady State Analysis

The thermal evolution of the convecting and radiating reactive slab attains a steady state for a given set of parameter values, and (5)–(7) then become

$$\begin{aligned} \frac{d^2 \theta}{dy^2} + \lambda \left( (1 + \gamma\theta)^m \left[ e^{\theta/(1+\gamma\theta)} + \beta e^{(r\theta)/(1+\gamma\theta)} \right] \right. \\ \left. - Ra \left[ (\gamma\theta + 1)^4 - 1 \right] \right) = 0, \end{aligned} \quad (11)$$

with

$$\frac{d\theta}{dy}(0) = \text{Bi}_1 \theta(0), \quad \frac{d\theta}{dy}(1) = -\text{Bi}_2 \theta(1), \quad (12)$$

where  $Ra = N_r/\lambda$  and (11) and (12) represent a boundary value nonlinear problem. This nonlinear nature precludes its exact solution. Using regular perturbation technique, it is

convenient to form a power series expansion in the Frank-Kamenetskii parameter  $\lambda$ ; that is,

$$\theta = \sum_{i=0}^{\infty} \theta_i \lambda^i. \quad (13)$$

Substituting the solution series (13) into (11) and (12) and collecting the coefficients of like powers of  $\lambda$ , we obtained and solved the equations for the coefficients of solution series iteratively. The solution for the temperature field is given in the appendix. Using computer symbolic algebra package (MAPLE), we obtained the first twenty terms of the solution series as well as the series for slab surface heat transfer rate  $\text{Nu} = -\theta'(1)$ . We are aware that this power series solution is valid for very small parameter values. In order to extend the usability of the solution series beyond small parameter values, a special type of Hermite-Padé approximant based on series summation and improvement technique is employed as illustrated in the following section (Hunter and Baker [14]; Makinde [9]).

## 5. Thermal Stability Analysis

The thermal stability properties and the onset of thermal runaway in the convecting and radiating reactive slab under consideration are characterized by the estimation of critical regimes separating the regions of explosive and nonexplosive chemical reactions. In order to achieve this goal, we employ a special type of Hermite-Padé approximation technique [8, 9, 14]. Suppose that the partial sum

$$U_{N-1}(\lambda) = \sum_{i=0}^{N-1} a_i \lambda^i = U(\lambda) + O(\lambda^N) \quad \text{as } \lambda \rightarrow 0 \quad (14)$$

is given. It is important to note here that (14) can be used to approximate any output of the solution of the problem under investigation (e.g., the series for the surface heat flux  $\text{Nu} = -\theta'(1)$  since everything can be Taylor expanded in the given small parameter). Assume that  $U(\lambda)$  is a local representation of an algebraic function of  $\lambda$  in the context of nonlinear problems; we construct an expression of the form

$$F_d(\lambda, U) = \sum_{i=1}^d \sum_{k=0}^i f_{i-k,k} \lambda^{i-k} U^k, \quad (15)$$

of degree  $d \geq 2$ , such that

$$\frac{\partial F_d}{\partial U}(0, 0) = 1, \quad F_d(\lambda, U_N) = O(\lambda^{N+1}), \quad \text{as } \lambda \rightarrow 0. \quad (16)$$

The requirement (16) reduces the problem to a system of  $N$  linear equations for the unknown coefficients of  $F_d$ . The entries of the underlying matrix depend only on the  $N$  given coefficients  $a_n$ , and we shall take  $N = (d^2 + 3d - 2)/2$ , so that the number of equations equals the number of unknowns. The polynomial  $F_d$  is a special type of Hermite-Padé approximant and is then investigated for bifurcation and thermal criticality conditions using Newton diagram (Vainberg and Trenogin [15]).

TABLE 1: Computations showing the procedure rapid convergence for  $\text{Bi}_1 = \text{Bi}_2 = 10$ ;  $N_r = m = \beta = \gamma = r = 0$ .

$d$	$N$	$\text{Nu} = -\theta'(1)$	$\lambda_{cN}$
2	4	0.29887011	2.4765973
3	8	0.29888521	2.4768101
4	13	0.29888146	2.4768124
5	19	0.29888146	2.4768124

TABLE 2: Computations showing the critical values of the reaction rate parameter  $\text{Bi}_1 = 1$ .

$N_r$	$\text{Bi}_2$	$\beta$	$r$	$m$	$\gamma$	$\text{Nu}$	$\lambda_c$
1	1	0.1	0.1	0.5	0.1	1.0825	0.8179
5	1	0.1	0.1	0.5	0.1	1.1927	1.5468
10	1	0.1	0.1	0.5	0.1	1.2486	2.4632
1	5	0.1	0.1	0.5	0.1	2.3721	1.3129
1	100	0.1	0.1	0.5	0.1	3.0569	1.6614
1	1	0	0.1	0.5	0.1	1.0358	0.8476
1	1	1	0.1	0.5	0.1	1.3910	0.6415
1	1	0.1	1	0.5	0.1	1.0421	0.7706
1	1	0.1	2	0.5	0.1	0.8331	0.6669
1	1	0.1	0.1	0	0.1	1.1662	0.8713
1	1	0.1	0.1	-2	0.1	1.7903	1.1941
1	1	0.1	0.1	0.5	0.2	4.2475	1.3531
1	1	0.1	0.1	0.5	0.4	1.4386	2.6350

## 6. Results and Discussion

We have assigned numerical values to the parameters encountered in the problem in order to get a clear insight into the thermal development in the system. At initial stage, the uniform temperature of the slab is assumed and parameter  $b = 0$ . It is very important to note that  $\beta = 0$  corresponds to a one-step chemical reaction case; an increase in the value  $\beta > 0$  signifies an increase in the two-step chemical reaction activities in the system. The thermal stability procedure above is applied on the first 19 terms of the solution series, and we obtained the results as shown in Tables 1 and 2. Table 1 shows the rapid convergence of the dominant singularity  $\lambda_c$ , that is, the value of thermal criticality in the system together with its corresponding slab surface heat transfer rate  $\text{Nu}$  as the number of series coefficients utilized in the approximants increases. It is noteworthy that the value of the critical regime for thermal stability when  $\beta = 0$  is perfectly in agreement with the one reported in Makinde [8] for a one step exothermic chemical reaction scenario.

Table 2 illustrates the variation in the values of thermal criticality conditions ( $\lambda_c$ ) for different combination of thermophysical parameters. The magnitude of thermal criticality decreases with increasing values of two-step reaction rate parameter  $\beta > 0$  and the activation energies ratio parameter  $r > 0$ . This implies that thermal instability and successive explosion are enhanced by two-step exothermic reaction and higher second step activation energy. At very large activation energy ( $\gamma = 0$ ), thermal explosion criticality is independent of the type of reaction as shown in (5). For moderately value

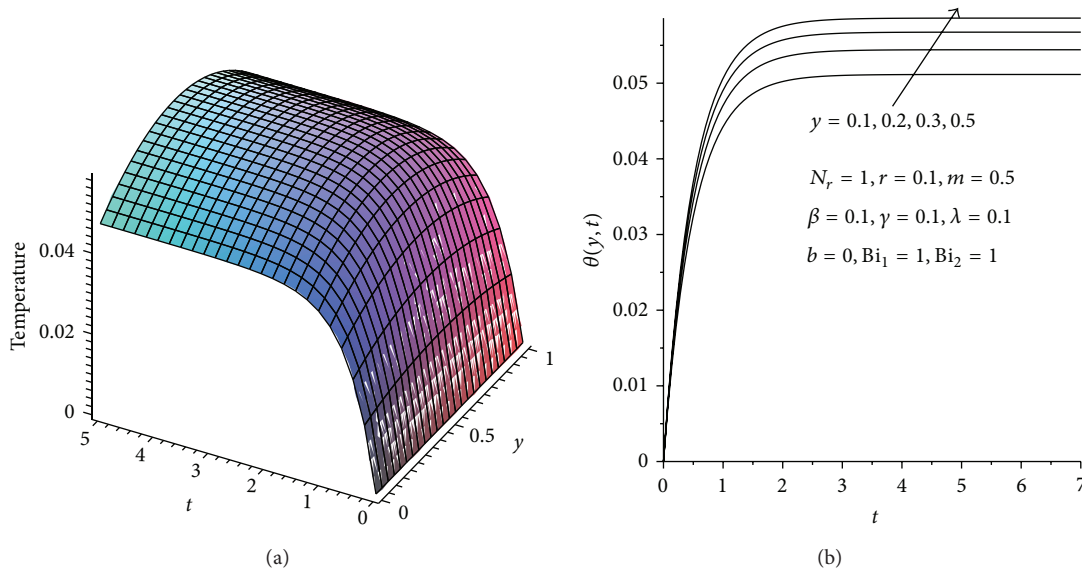


FIGURE 3: Temperature profiles with increasing time.

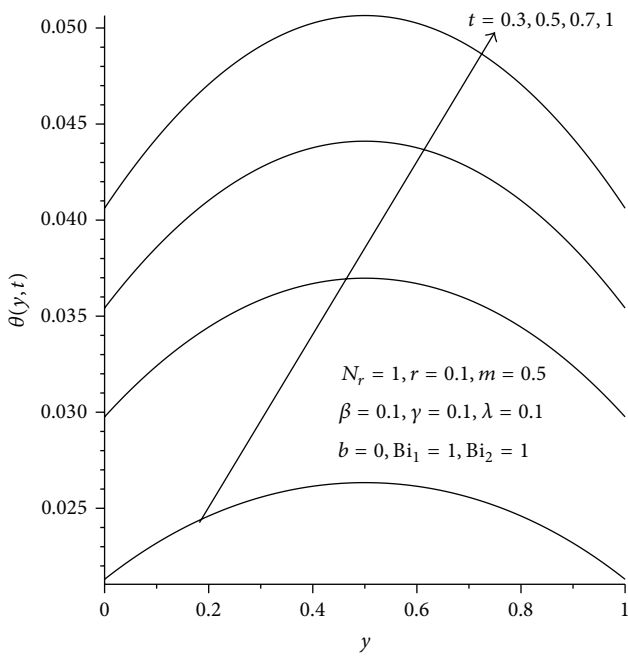


FIGURE 4: Transient effects on temperature profiles.

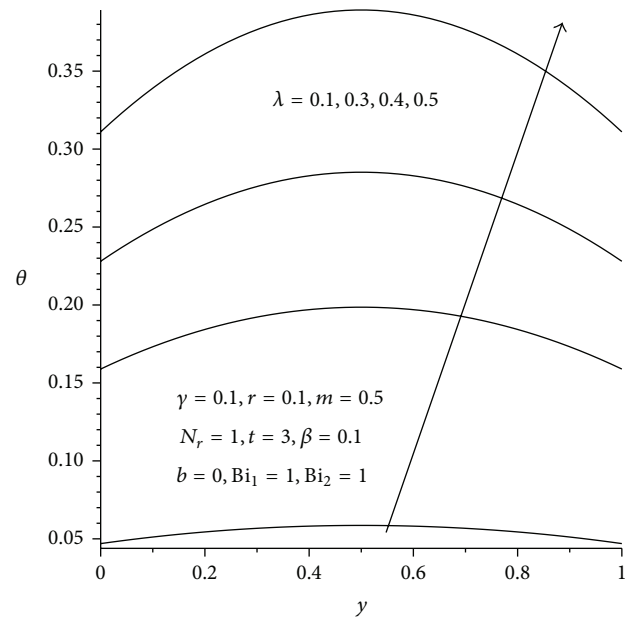


FIGURE 5: Effects of increasing reaction rate on temperature profiles.

of activation energy, the criticality varies from one type of reaction to another. It is interesting to note from Table 2 that explosion in bimolecular reaction will occur faster than in Arrhenius and sensitized reactions. This can be attributed to the lower thermal criticality value of bimolecular reaction. Moreover, it is interesting to note that the magnitude of thermal criticality increases with an increase in convective and radiative heat loss as well as a decrease in the activation energy (i.e.,  $N_r > 0, Bi_2 > 0$ , and  $\gamma > 0$ ), thus preventing the early development of thermal runaway and enhancing thermal stability in the system as expected.

6.1. Effects of Parameter Variation on Temperature Profiles.

Figures 3(a), 3(b), and 4 illustrate the evolution of the temperature field in the reactive slab. For fixed values of various thermophysical parameters, the slab temperature increases rapidly with time until it attains its steady state value as shown in Figure 3(b). It is observed that for the given set of parameter values, a steady state temperature reaches at time  $t = 2$ . Generally the temperature is maximum along the slab centerline and minimum at the surface due to convective and radiative heat loss, thus satisfying the prescribed boundary conditions. In Figures 5 and 6, it is observed that the slab temperature generally increases with

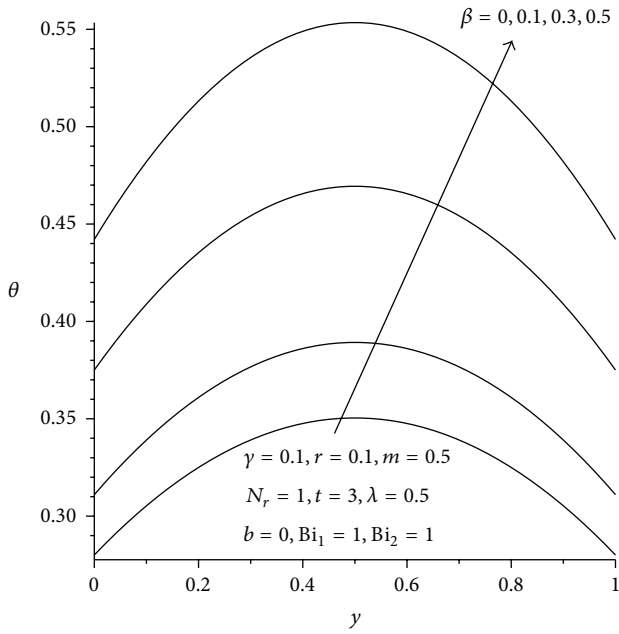


FIGURE 6: Effects of increasing two-step reaction parameter on temperature profiles.

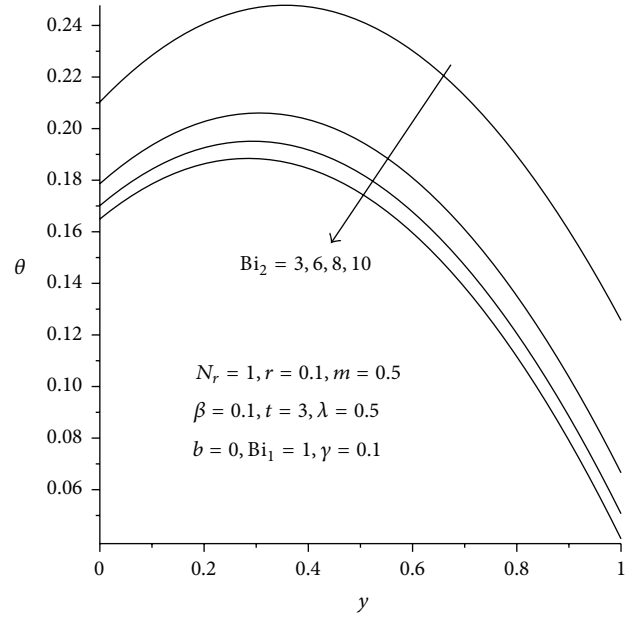


FIGURE 8: Effects of asymmetrical convective heat loss on temperature profiles.

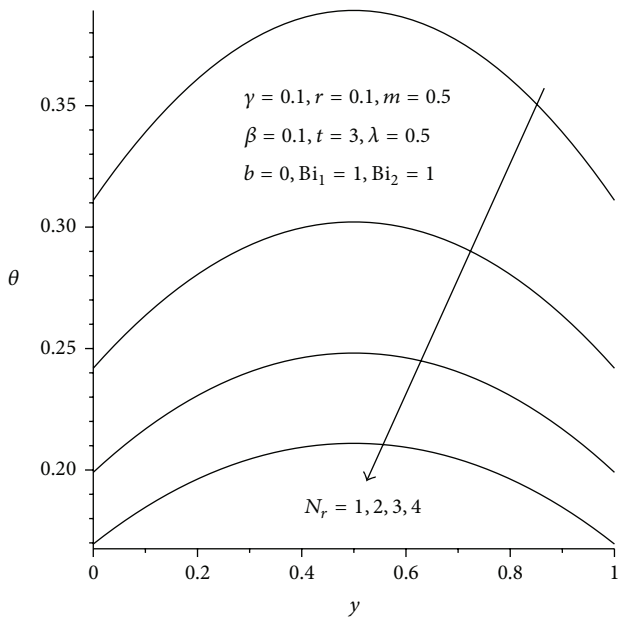


FIGURE 7: Effects of increasing radiative heat loss on temperature profiles.

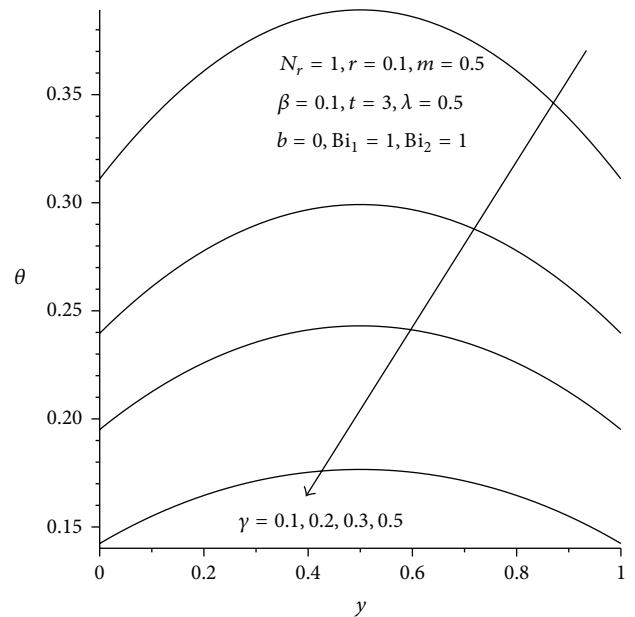


FIGURE 9: Effect of increasing activation energy parameter on temperature profiles.

increasing value of Frank-Kamenetskii parameter ( $\lambda$ ) and two-step reaction parameter ( $\beta$ ). This can be attributed to an increase in the rate of internal heat generation activities due to chemical kinetics in the system. Figures 7 and 8 illustrate the effects of heat loss on the reactive slab due to radiation and asymmetric convective cooling. As expected, a general decrease in the slab temperature is observed with increasing parameter values of  $N_r$ ,  $Bi_2$ . Similar trend is observed in Figure 9 with a decrease in the slab activation energy. As the

value of  $\gamma > 0$  increases, the slab temperature decreases. This can be attributed to an increase in the slab thermal resistance. The expression for power law nonlinear regression with respect to the slab temperature and the parameter variation is obtained from the numerical data especially along the slab centreline  $y = 0.5$  when  $Bi_1 = 1$  as  $\theta = c_0 t^{c_1} \lambda^{c_2} \beta^{c_3} N_r^{c_4} Bi_2^{c_5} \gamma^{c_6}$ , where  $c_0 = 0.21$ ,  $c_1 = 0.14$ ,  $c_2 = 1.73$ ,  $c_3 = 0.12$ ,  $c_4 = -0.16$ ,  $c_5 = -0.37$ , and  $c_6 = -0.25$ . This also confirmed our results that the slab temperature decreases with an increase



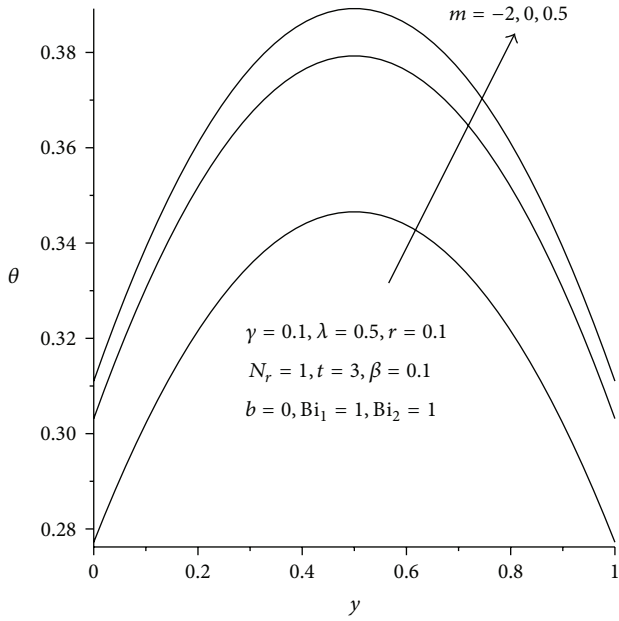


FIGURE 10: Effect of reaction types on temperature profiles.

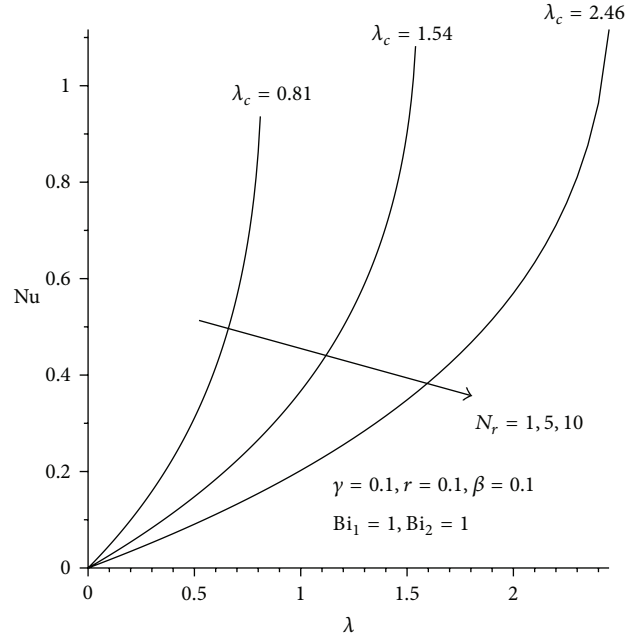


FIGURE 12: Effect of increasing radiative heat loss on critical value of  $\lambda_c$ .

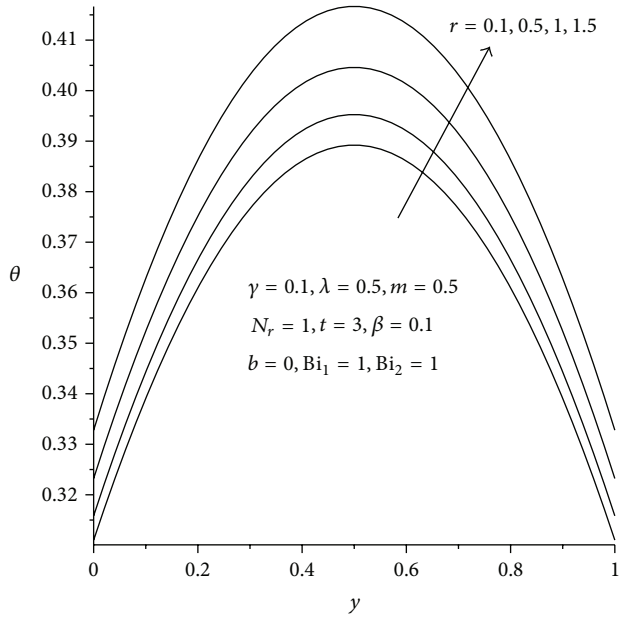


FIGURE 11: Effects of increasing activation energy ratio parameter on temperature profiles.

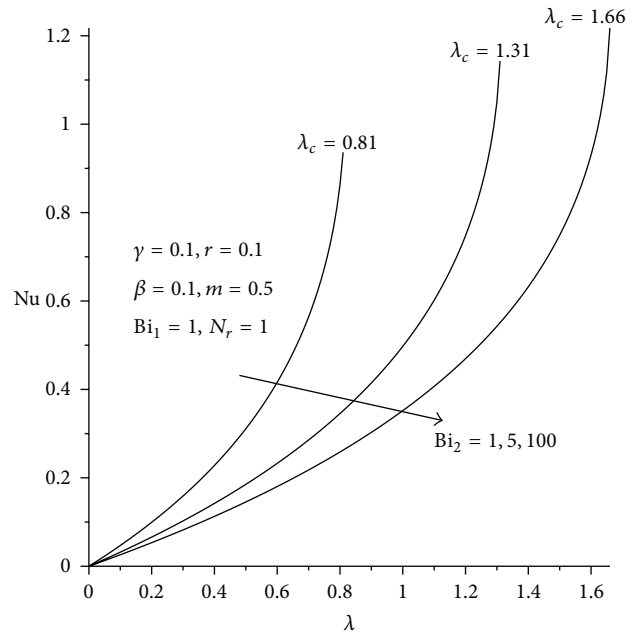


FIGURE 13: Effect of increasing convective heat loss on critical value of  $\lambda_c$ .

in the activation energy parameter (i.e., a decrease in the slab activation energy) and an increase in both radiative and convective heat losses. However, the temperature increases with a rise in the exothermic reaction rate and two-step reaction parameter.

Figure 10 shows that the slab temperature is highest during bimolecular reaction and lowest for sensitized reaction, hence confirming the result highlighted in the Table 2. In Figure 11, it is observed that the slab temperature increases with an increase in the two-step reaction activation energy

ratio ( $r$ ). Interestingly, an increase in  $r > 0$  indicates that the activation energy of the second step reaction is higher than that of the first step reaction, leading to an increase in the internal heat generated within the slab.

6.2. Effects of Parameter Variation on Slab Thermal Stability. Figures 12–16 illustrate the effects of parameter variation on

the thermal stability of the slab under a two-step reaction scenario. It represents the variation of slab surface heat transfer rate with the Frank-Kamenetskii parameter ( $\lambda$ ) defined as

$$Nu = \frac{aE_1 q_w}{kRT_\infty^2} = -\theta'(1), \quad (17)$$

where  $q_w = -k\partial T/\partial \bar{y}$  at  $\bar{y} = a$ . It is well known that thermal instability do occur whenever the rate of internal heat generation due to exothermic reaction within a system is higher than the rate at which the system loses heat to the ambient. This invariably leads to accumulation of heat within the system, and consequently thermal runaway developed. In particular, for every a fixed set of thermophysical parameters at steady state, there is a critical value  $\lambda_c$  (see Table 2) such that, for  $0 \leq \lambda < \lambda_c$ , the slab is thermally stable. When  $\lambda_c < \lambda$ , the system becomes thermally unstable leading to thermal runaway. In Figures 12 and 13, it is observed that the thermal stability interval for parameter value  $\lambda$  increases with an increase in convective and radiative heat loss to the ambient as expected, since this reduces the accumulation of heat within the reacting slab. Figure 14 shows that the thermal stability interval for parameter value  $\lambda$  decreases with an increase in two-step reaction parameter leading to early occurrence on thermal runaway in the system. Interestingly, this shows clearly that a multistep exothermic reaction is more thermally unstable in comparison to a one step reaction process. As  $\gamma$  increases due to a decrease in the slab activation energy, thermal stability interval for parameter value  $\lambda$  increases as shown in Figure 15. It implies that less volatile reactive materials are more thermally stable as compared to highly volatile reactive materials. In Figure 16, it is observe that thermal instability in the slab will occur faster during bimolecular reaction as compared to Arrhenius and sensitized reactions. This is noteworthy that although the chemical reaction is exothermic, early development of thermal runaway in the system depends on the type of reaction process due to the temperature dependent preexponential factor. Moreover, the thermal criticality results depicted in Figures 12–16 are in perfect agreement with the one shown in Table 2.

### 7. Conclusion

The combined effects of asymmetric convective and radiative heat loss on a two-step exothermic reactive slab, taking the diffusion of the reactant into account and assuming a temperature dependent variable preexponential factor, have been investigated. Both transient and steady state of reactive slab scenario are examined. The nonlinear governing equation is solved numerically using a semidiscretization finite difference scheme and a perturbation technique coupled with a special type of Hermite-Padé approximants. Our results can be summarized as follows.

- (i) Increase in  $\lambda$ ,  $\beta$ ,  $r$ , and  $m$  increases the slab temperature profile, while increase in  $\gamma$ ,  $N_r$ ,  $Bi_1$ , and  $Bi_2$  decreases slab temperature profiles.
- (ii) A critical value  $\lambda_c$  exists such that for  $0 \leq \lambda < \lambda_c$ , the slab is thermally stable and for  $\lambda > \lambda_c$  the slab is thermally, unstable leading to thermal runaway.

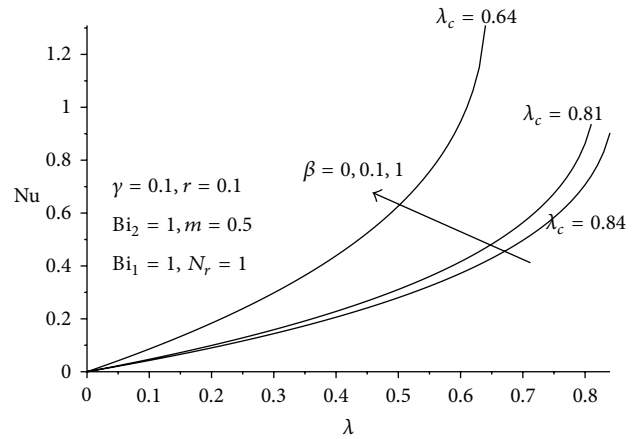


FIGURE 14: Effect of two-step reaction parameter on critical value of  $\lambda_c$ .

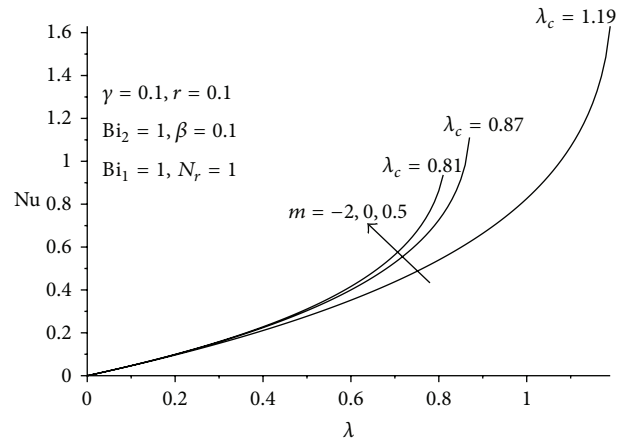


FIGURE 15: Effect of reaction type on parameter on critical value of  $\lambda_c$ .

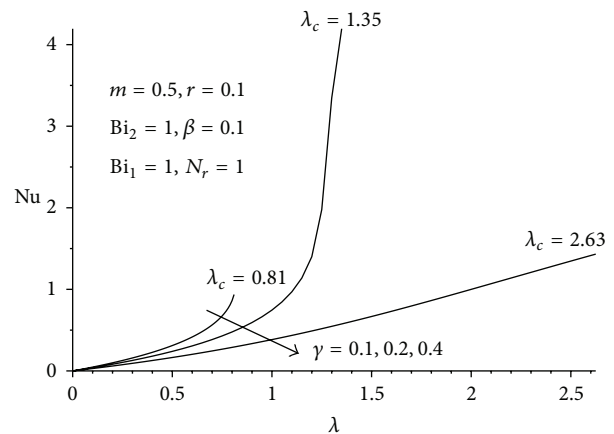


FIGURE 16: Effect of activation energy parameter on critical value of  $\lambda_c$ .



- (iii) Increase in  $\beta$ ,  $r$ , and  $m$  increases the onset of thermal instability, while increase in  $\gamma$ ,  $N_r$ ,  $Bi_1$ , and  $Bi_2$  enhanced slab thermal stability.

## Conflict of Interests

The authors declare that there is no conflict of interests regarding the publication of this paper.

## Acknowledgment

The authors would like to thank the National Research Foundation (NRF) of South Africa for their generous financial support.

## References

- [1] J. Bebernes and D. Eberly, *Mathematical Problems from Combustion Theory*, Springer, New York, NY, USA, 1989.
- [2] F. A. Williams, *Combustion Theory*, Benjamin & Cuminy publishing, Menlo Park, Calif, USA, 2nd edition, 1985.
- [3] D. A. Frank Kamenetskii, *Diffusion and Heat Transfer in Chemical Kinetics*, Plenum Press, New York, NY, USA, 1969.
- [4] O. D. Makinde, "Thermal stability of a reactive viscous flow through a porous-saturated channel with convective boundary conditions," *Applied Thermal Engineering*, vol. 29, no. 8-9, pp. 1773–1777, 2009.
- [5] F. S. Dainton, *Chain Reaction: An Introduction*, John Wiley & Sons, New York, NY, USA, 1960.
- [6] Z. G. Szabo, *Advances in Kinetics of Homogeneous Gas Reactions*, Methuen and Company, Great Britain, UK, 1964.
- [7] G. I. Barenblatt, J. B. Bell, and W. Y. Crutchfield, "The thermal explosion revisited," *Proceedings of the National Academy of Sciences of the United States of America*, vol. 95, no. 23, pp. 13384–13386, 1998.
- [8] O. D. Makinde, "Exothermic explosions in a slab: a case study of series summation technique," *International Communications in Heat and Mass Transfer*, vol. 31, no. 8, pp. 1227–1231, 2004.
- [9] O. D. Makinde, "Hermite-Padé approach to thermal stability of reacting masses in a slab with asymmetric convective cooling," *Journal of the Franklin Institute*, vol. 349, no. 3, pp. 957–965, 2012.
- [10] N. N. Semenov, *Chemical Kinetics and Chain Reactions*, The Clarendon Press, Oxford, UK, 1935.
- [11] E. Balakrishnan, A. Swift, and G. C. Wake, "Critical values for some non-class A geometries in thermal ignition theory," *Mathematical and Computer Modelling*, vol. 24, no. 8, pp. 1–10, 1996.
- [12] O. D. Makinde, "On the thermal decomposition of reactive materials of variable thermal conductivity and heat loss characteristics in a long pipe," *Journal of Energetic Materials*, vol. 30, no. 4, pp. 283–298, 2012.
- [13] K. W. Morton and D. F. Mayers, *Numerical Solution of Partial Differential Equations: An Introduction*, Cambridge University Press, 2005.
- [14] D. L. Hunter and G. A. Baker Jr., "Methods of series analysis. III. Integral approximant methods," *Physical Review B*, vol. 19, no. 7, pp. 3808–3821, 1979.
- [15] M. M. Vainberg and V. A. Trenogin, *Theory of Branching of Solutions of Nonlinear Equations*, Wolters-Noordhoff B.V., Leyden, Mass, USA, 1974.